RARE METALS
Vol. 30, No. 6, Dec 2011, p. 681
DOI: 10.1007/s12598-011-0449-4

Thermal behaviors and growth of reduced ferronickel particles in carbon-laterite composites

HUANG Donghua[a, b], ZHANG Jianliang[a], MAO Rui[a], and CAO Mingming[a]

[a] *School of Metallurgical and Ecological Engineering, State Key Laboratory of Advanced Metallurgy, University of Science and Technology Beijing, Beijing 100083, China*
[b] *Journals Publishing Center, University of Science and Technology Beijing, Beijing 100083, China*

Received 28 March 2011; received in revised form 25 May 2011; accepted 10 June 2011

Abstract

The thermal behaviors of single laterite ore and graphite-laterite mixtures were investigated by thermogravimetry (TG), derivative thermogravimetry (DTG), and differential thermal analysis (DTA). Four mass loss steps maximized at about 78, 272, 583, and 826°C are observed for the laterite ore, representing the vaporization of free water, the dehydroxylation of goethite, the decomposition of serpentines, and the second dehydroxylation of serpentines, respectively. The reduction reactions of the graphite-laterite mixtures start at around 700°C and can be divided into three major temperature regions. Coal-laterite composites with an addition of 10 wt.% CaO were roasted at 1100-1350°C for 30 min, and the reduced samples were characterized by X-ray diffraction (XRD) and scanning electron microscopy (SEM). The results indicate that the reduction reactions proceed more completely at higher temperatures. The growth of the reduced ferronickel particles is greatly influenced by the roasting temperature. Obvious growth of the reduced ferronickel particles appears with the formation of worm-like crystals for the sample reduced at 1250°C, and spheric particles are observed for the sample reduced at 1300°C. When the reduction temperature increases to 1350°C, the reduced ferronickel particles agglomerate to ferronickel granules of 3-8 mm in diameter. The main elements in the granules include iron, nickel, chromium, carbon, and sulfur, with the content of nickel and that of iron of 9.08 wt.% and 85.21 wt.%, respectively.

Keywords: laterite; ferronickel granules; dehydration; reduction; thermal analysis

1. Introduction

Laterites comprise about 70% of world land based nickel resources, but they account for only about 40% of the world nickel production, since the concentration of nickel in laterites is relatively low [1-2]. In recent years, with the depletion of high-grade nickel ores, much attention has been focused on the utilization of low-grade laterites [3].

The established industrial processes for nickel recovery from laterites mainly include the rotary kiln-electric furnace (RK-EF) process [4-5], high-pressure acid leaching (HPAL) process [6-7], and the reductive roast-ammonia leaching (Caron) process [8-9]. The RK-EF process is a preferred process route for treatment of garnieritic type ores, but it requires high grade ores and is energy intensive [10]. The HPAL process requires ores that are predominantly limonitic, and it has severe scale and corrosion problems and needs high maintenance costs [6]. The Caron process can be used for limonitic ores or a mixture of limonite and saprolite. But it suffers from the disadvantages of low nickel recovery, high energy consumption, and reagent requirements [6, 11].

The Oheyama process, which produces ferronickel granules by direct reduction of garnierite ore in a rotary kiln, is considered to be a low-cost ferronickel process with the advantages of low energy consumption and using coal rather than expensive electric power as main energy source. Moreover, the produced ferronickel granules with little content of impurities can be well utilized as the raw material for stainless steel making [12-13]. In this process, calcining and reduction of metal oxides are conducted at a sufficiently high temperature to cause the partial melting of the calcine, thus permitting the growth of ferronickel granules. The calcined material is then water-quenched and ground, and the metal granules are magnetically separated from the gangue [5]. The main problem of this process is ring growth inside the kiln. Therefore, a fundamental study focusing on the reduction of oxides and agglomeration of the metal particles is needed for the establishment of a successful practice. In this paper, the thermal dehydration and reduction behaviors of graphite-laterite ore mixtures were investigated. Meanwhile,

Corresponding author: ZHANG Jianliang **E-mail:** jl.zhang@metall.ustb.edu.cn

the growth of reduced ferronickel particles in a coal-laterite composite was studied.

2. Experimental

2.1. Materials

The laterite ore used in this work originated from Indonesia. The typical chemical analysis of the ore is shown in Table 1. The contents of silicon and magnesium in the ore were high, whereas the contents of iron and cobalt were low. Fig. 1 shows the X-ray diffraction (XRD) spectrum of the raw ore. The main minerals identified include serpentine group minerals (clinochrysotile ($Mg_3Si_2O_5(OH)_4$), pecoraite ($Ni_3Si_2O_5(OH)_4$), nepouite ($(Ni,Mg)_3Si_2O_5(OH)_4$), lizardite ($(Mg,Fe)_3Si_2O_5(OH)_4$), and kaolinite ($Al_2Si_2O_5(OH)_4$)), hematite (Fe_2O_3), goethite (FeO(OH)), and quartz (SiO_2). Prior to the experiments, the ore was dried in an oven at 105°C for 3 h and ground with 80% of the particles less than 74 μm.

Table 1. Chemical compositon of the laterite ore wt.%

Ni	TFe	FeO	SiO_2	CaO	MgO	Al_2O_3	Co	Cr	S	P
1.59	16.86	0.57	39.9	1.29	15.0	3.19	0.02	0.47	0.019	0.004

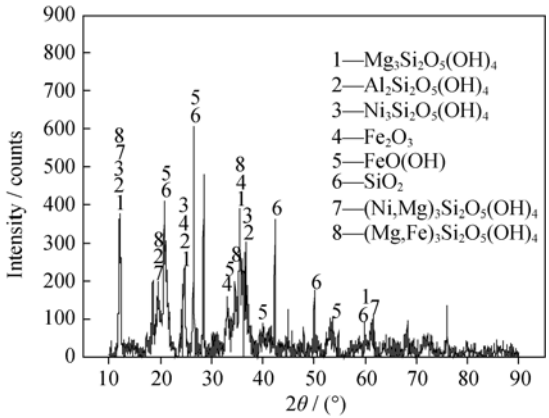

Fig. 1. XRD spectrum of the laterite ore.

Bituminous coal with particle sizes less than 180 μm and graphite reagent with 95% of the particles less than 180 μm were used as carbonaceous reductant. The carbon content, volatile content, and ash content of dry basis of the bituminous coal were 57.52 wt.%, 34.52 wt.%, and 7.96 wt.%, respectively.

2.2. Thermal analysis

The thermal properties of single laterite ore and graphite-ore mixtures were analyzed by thermogravimetry (TG) using a Mettler Toledo TGA/SDTA 851e analyzer. The thermal analysis of a graphite-precalcined ore mixture (the ore was precalcined at 900°C for 2 h in a muffle furnace (SX-8-16)) was also carried out. The C/O molar ratios of the graphite-ore mixtures were 1.0, 1.2, and 1.4, and that of the graphite-precalcined ore mixture was 1.2. Samples of about 20 mg were heated from 25 to 1300°C with a heating rate of 10°C/min in an argon flow of 30 mL/min. The corresponding differential thermal analysis (DTA) and derivative thermogravimetry (DTG) curves were also measured.

2.3. High-temperature reduction experiment

Powders of laterite ore, coal, and CaO (10 wt.%) with a C/O molar ratio of 1.3 were well mixed and press-shaped to composite samples of 20 mm in diameter and 20 mm in height. The samples were dried and placed in graphite crucibles covered with a layer of fine coke (2 mm deep) and roasted in the muffle furnace at 1100-1350°C for 30 min. The reduced samples were isolated from air during cooling.

The microstructures of the reduced composites were observed using a scanning electron microscope (SEM) equipped with an energy dispersive spectrometer (EDS). The phase compositions of the raw ore, precalcined ore, and reduced composites were analyzed using X-ray diffraction (XRD).

3. Results and discussion

3.1. Thermal analysis

Fig. 2 shows the TG curve of the laterite ore. The corresponding DTG and DTA curves are also shown. There are four mass loss steps in the TG curve. The first mass loss step begins at 47°C and is maximized at 78°C, with a significant endothermic peak in the DTA curve. This step represents the vaporization of free water. The second mass loss step initiates at 250°C and is maximized at 272°C, also accompanied with an endothermic peak in the DTA curve. This endothermic step is assigned to the dehydroxylation of goethite (FeO(OH)) with the formation of hematite. Carlson and Schwertmann reported a dehydroxylation temperature of 385°C for highly crystalline goethite [14]. The dehydroxylation temperature of fine-grained and poorly crystalline goethite is always lower than that of coarse-grained highly crystalline goethite [15]. The relatively low dehydration temperature of this work, 272°C, indicates poorly crystalline structure of goethite. The third mass loss step starts at 533°C and has a maximum mass loss rate at 583°C, which is attributed to the decomposition of serpentines. The fourth mass loss step occurring between 755 and 864°C and maximized

at 826°C may be attributed to the second dehydroxylation stage of serpentines [16-17]. The total mass loss in the temperature range of 25 to 1300°C is 12%. The exothermic peak at 820°C is due to the crystallization of forsterite [18], which is a dehydration product of serpentine.

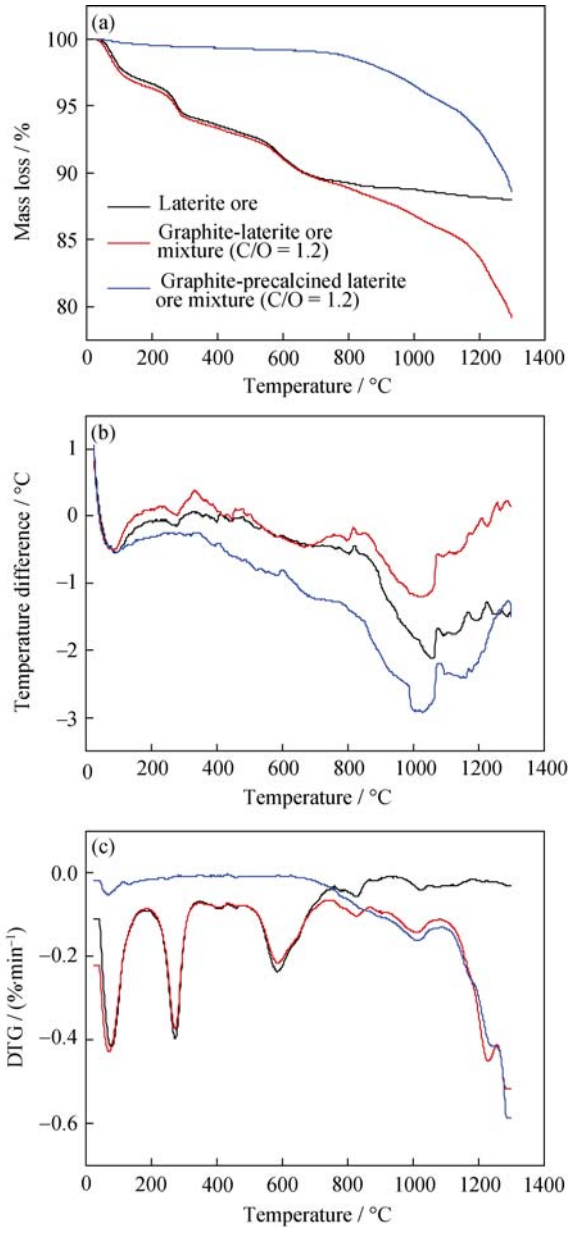

Fig. 2. TG (a), DTA (b), and DTG (c) curves of laterite ore, graphite-laterite ore mixture, and graphite-precalcined laterite ore mixture.

The TG-DTA-DTG curves of the graphite-precalcined ore mixture with a C/O molar ratio of 1.2 are also presented in Fig. 2. The first endothermic peak at approximately 92°C, corresponding to a mass loss of 0.3%, identifies the presence of minor free water. As the ore was precalcined, it is believed that this sample most likely absorbed some amounts of atmospheric moisture during handling. The mass loss associated with laterite ore reduction commences at about 700°C. The mass loss curve for temperatures above this range can be divided into three temperature regions of 700-1090, 1090-1258, and 1258-1300°C. The mass loss is associated with the reduction of nickel and iron oxides and the gasification of carbon, which are largely endothermic. The reduction reactions have not reached equilibrium at 1300°C.

The mass loss curve of the graphite-ore mixture exhibits similarities with that of the single laterite ore prior to 700°C. Removal of free water, dehydroxylation of goethite, and decomposition of kaolinite and serpentines are the dominant reactions for the mixture, with mass losses being similar to those of single laterite ore. Above 864°C, where the mass loss owing to dehydration is minor, the mass loss curve of the graphite-ore mixture is similar to that of the graphite-precalcined ore mixture. Both dehydration and reduction reactions contribute to the mass loss in the temperature range of 700-864°C.

Fig. 3 shows the TG and DTG curves of the graphite-ore mixtures with C/O molar ratios of 1.0, 1.2, and 1.4. The three mixtures exhibit similar TG and DTG curves prior to 1000°C. The transition temperatures T_1 and T_2 decrease with an increase in C/O molar ratio. The reason is that with an increase in C/O molar ratio in the mixtures, the concentra-

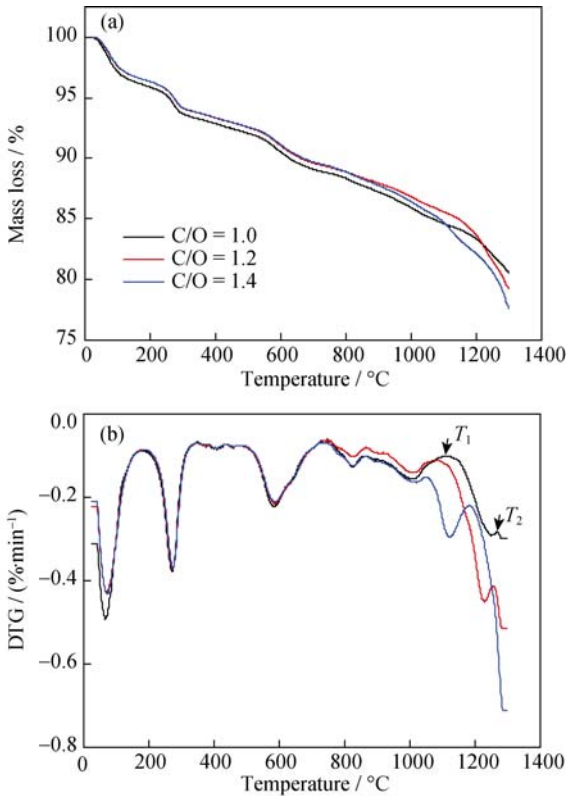

Fig. 3. TG (a) and DTG (b) curves of graphite-laterite ore mixtures with C/O molar ratios of 1.0, 1.2, and 1.4.

tion of CO generated by carbon gasification reaction increases, driving the reduction reactions toward lower temperatures.

In the initial stage of laterite ore reduction, nickel and iron oxides react with solid carbon:

$$NiO + C = Ni + CO \quad (1)$$

$$3Fe_2O_3 + C = 2Fe_3O_4 + CO \quad (2)$$

$$Fe_3O_4 + C = 3FeO + CO \quad (3)$$

$$FeO + C = Fe + CO \quad (4)$$

Reductant CO gas is generated by carbon gasification reaction when the required temperature for the gasification reaction is attained:

$$CO_2 + C = 2CO \quad (5)$$

Then the reductions occur by gaseous phases:

$$NiO + CO = Ni + CO_2 \quad (6)$$

Hematite is reduced to iron in three sequential steps,

$$3Fe_2O_3 + CO = 2Fe_3O_4 + CO_2 \quad (7)$$

$$Fe_3O_4 + CO = 3FeO + CO_2 \quad (8)$$

$$FeO + CO = Fe + CO_2 \quad (9)$$

It is rather difficult to associate the individual reaction with each temperature region, as it is expected that the reduction is cross-linked and interrelated.

3.2. XRD analysis

Fig. 4 shows the XRD spectrum of the laterite ore calcined at 900°C for 2 h in a muffle furnace. Complete dehydroxylation achieves under this condition. The minerals identified in the calcined ore include forsterite (Mg_2SiO_4), enstatite ($MgSiO_3$), nickel magnesium silicate ($(Ni,Mg)_2SiO_4$), metakaolinite ($Al_2Si_2O_7$), hematite (Fe_2O_3), and qurtze (SiO_2). Combined with the results in Fig. 1, it can be deduced that clinochrysotile decomposes to form forsterite and enstatite, kaolinite decomposes to form metakaolinite, and goethite dehydrates with the formation of hematite.

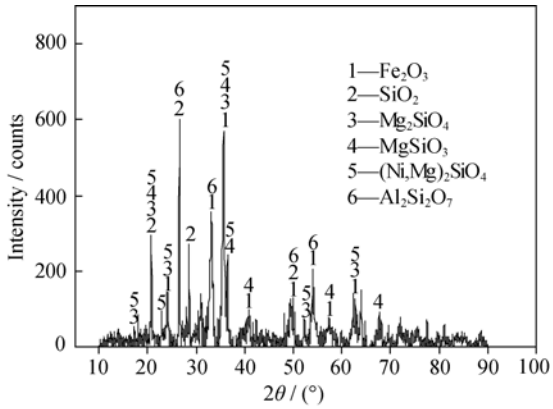

Fig. 4. XRD spectrum of the laterite ore calcined at 900°C for 2 h.

Fig. 5 shows the XRD spectra of the coal-laterite ore composites (with the addition of 10 wt.% CaO) roasted in temperature ranges of 1100-1300°C for 30 min. With an increase in reduction temperature, the peaks for kamacite phase become stronger. The wustite peak and $Ca(Fe,Mg)Si_2O_6$

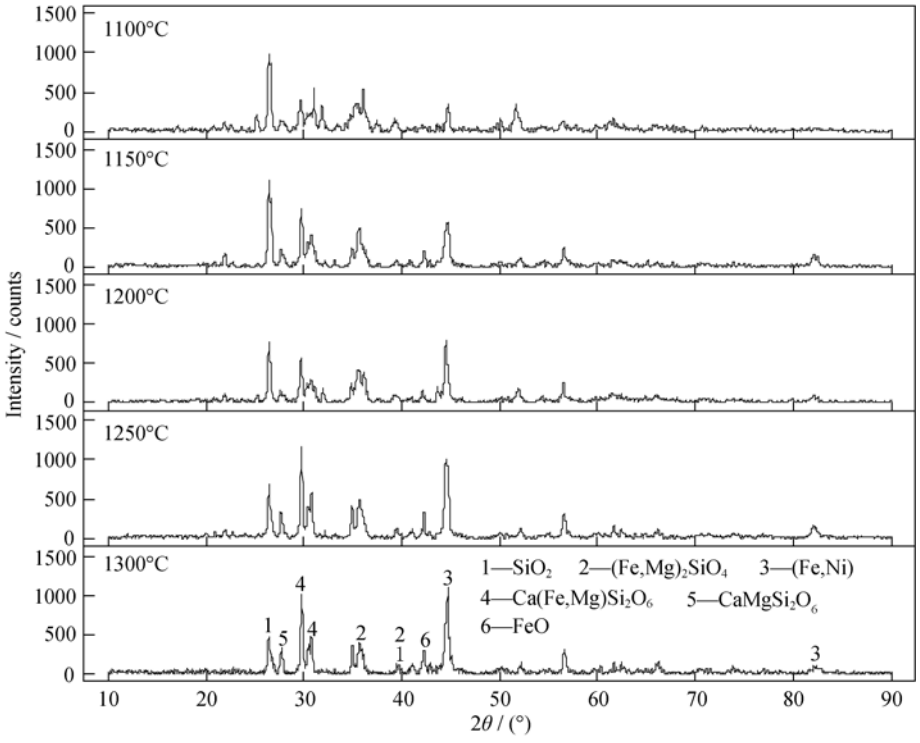

Fig. 5. XRD spectra of the coal-laterite ore composites roasted at different temperatures for 30 min.

peak become stronger with an increase in reduction temperature from 1100 to 1250°C but eventually weakens at 1300°C. The above-mentioned results suggest that the reduction reactions proceed more completely at higher temperatures. The quartz peak weakens with increasing temperature, whereas the diopside ($CaMgSi_2O_6$) peak becomes stronger, suggesting the possible participation of quartz in the reactions to form $Ca(Fe,Mg)Si_2O_6$ and diopside. The peak of fayalite ($(Fe,Mg)_2SiO_4$) is almost unchanged with the reduction temperature increasing from 1100 to 1250°C and slightly decreases at 1300°C.

3.3. SEM observations

Fig. 6 shows the cross-sectional SEM images of the coal-laterite composites reduced at 1100-1200°C for 30 min. The EDS results of regions a-f are shown in Table 2. As shown in Figs. 6(a) and 6(b), the sample reduced at 1100°C has a porous structure with the existence of cracks and pores, which might be due to the rapid gasification of bituminous coal. The black regions (region a in Fig. 6(a)) are carbon phase. The dark grey regions (region b in Fig. 6(a)) are carbon phase mixed with some MgO. Region c in Fig. 6(a) might be a mixture of olivine and quartz. Bright white re-

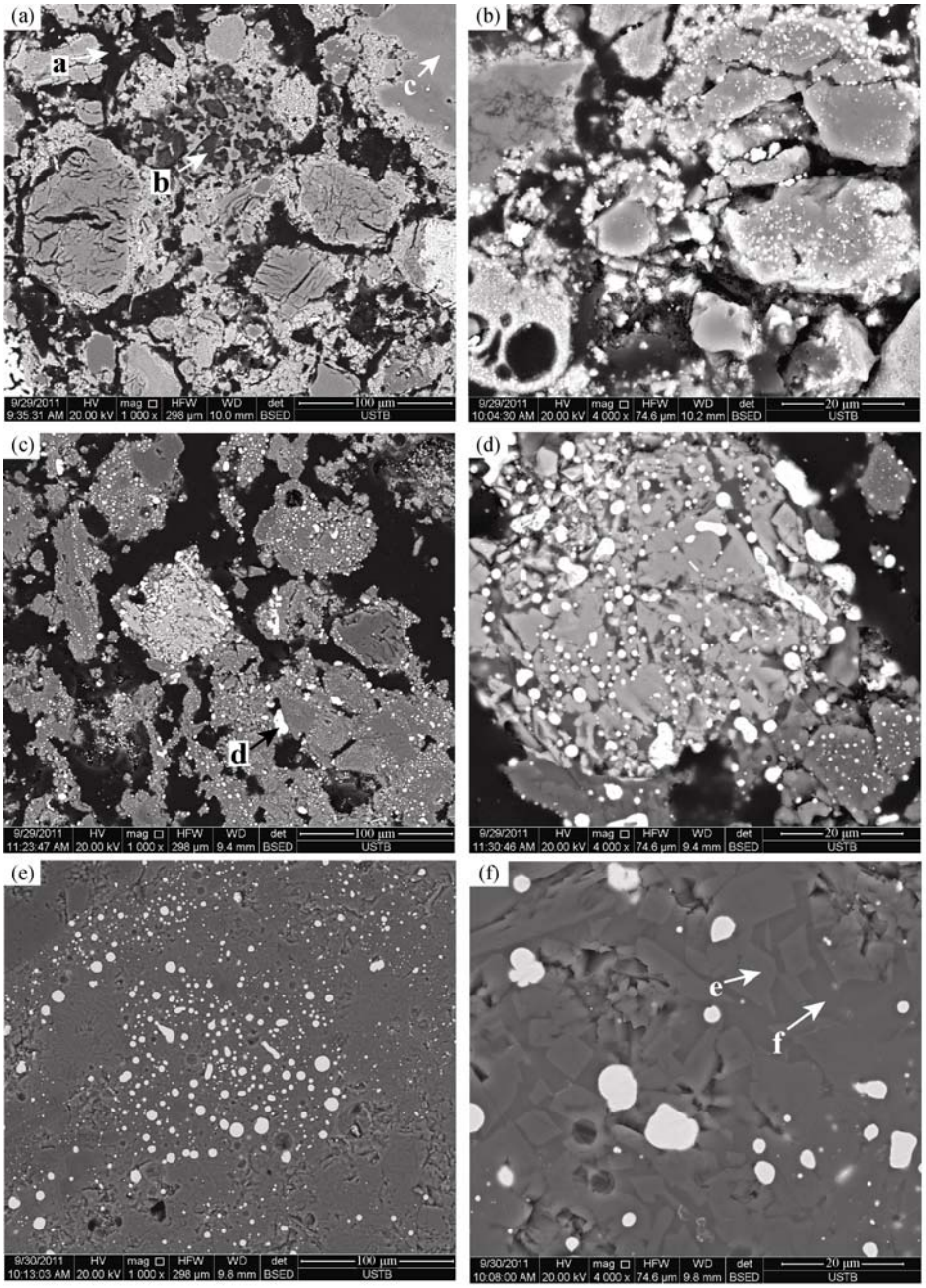

Fig. 6. SEM images of the cross sections of the coal-laterite composites roasted at 1100°C (a, b), 1150°C (c, d), and 1200°C (e, f) for 30 min at two different magnifications.

Table 2. Elemental composition of regions a-g marked in Figs. 6 and 7 analyzed by EDS wt.%

Region	C	O	Mg	Si	Ca	Fe	Ni	Co	Al	Cr	Mn
a in Fig. 6(a)	78.35	13.49		3.56		4.60					
b in Fig. 6(a)	43.26	18.62	29.61	1.59	2.10	4.24	0.59				
c in Fig. 6(a)		30.60	17.47	40.91		6.30	4.72				
d in Fig. 6(c)	6.23					62.64	26.17	4.96			
e in Fig. 6(f)		29.86	13.92	35.53	19.06				1.63		
f in Fig. 6(f)		31.29	7.60	36.56	14.77				9.78		
g in Fig. 7(b)	2.97					87.79	7.44			1.33	0.46

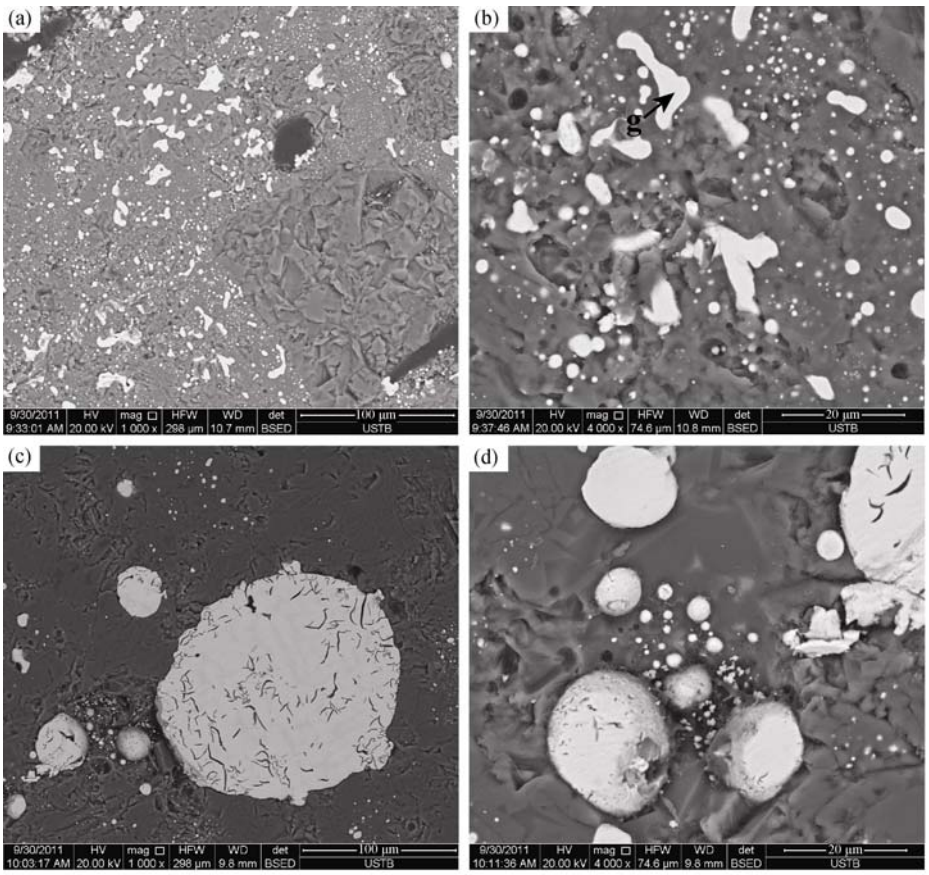

Fig. 7. SEM images of the cross sections of the coal-laterite composites roasted at 1250°C (a, b) and 1300°C (c, d) for 30 min at two different magnifications.

gions are reduced ferronickel phase, which are observed surrounding gangue and carbon particles. The appearance of ferronickel phase increases when the reduction temperature increases to 1150°C, as shown in Figs. 6(c) and 6(d). Region d in Fig. 6(c) is a ferronickel phase with some amounts of carbon and cobalt. Because iron oxides have not been totally reduced to metallic phase, the content of iron in the phase is quite low (62.64 wt.%), whereas that of nickel is rather high (26.17 wt.%). For the sample reduced at 1200°C, as shown in Figs. 6(e) and 6(f), the ferronickel phase grows to particles with a size of about 5-10 μm. Carbon particles are scarcely observed. Regions e and f in Fig. 6(f) are gangue minerals composed of MgO, CaO, SiO_2, and Al_2O_3. With the content of Al_2O_3 increasing, the color changes darker.

As the reduction temperature increases to 1250°C, the obvious connection and growth of the reduced ferronickel particles appear, and worm-like crystals with a length of about 15-20 μm are observed (Figs. 7(a) and 7(b)). Network voids are formed because of the consumption of solid carbon, which is beneficial to the diffusion and agglomeration of the reduced ferronickel particles. EDS analysis shows that region g in Fig. 7(b) is ferronickel alloy with the total contents of iron and nickel of 95.2 wt.%. Spheric particles with sizes of 20-150 μm are observed for the sample roasted at 1300°C, as shown in Figs. 7(c) and 7(d). The boundary between the reduced ferronickel particles and the slag is clear. When the reduction temperature increases to 1350°C, the carburization rate increases, causing the decrease of the

melting starting temperature. The agglomeration of the reduced ferronickel particles occurs in a semifused condition and ferronickel granules of 3-8 mm in diameter are formed, which can be seperated from the slag through comminuting and sieving.

Fig. 8 shows an SEM image of a ferronickel granule. The main elements in the granule include iron, nickel, chromium, carbon, and sulfur. Carbon is mainly solid-soluted in the alloy. In regions a to c in Fig. 8, with the color becoming darker, the content of carbon increases. Chemical analysis shows that the content of nickel and that of iron in the granules are 9.08 wt.% and 85.21 wt.%, respectively.

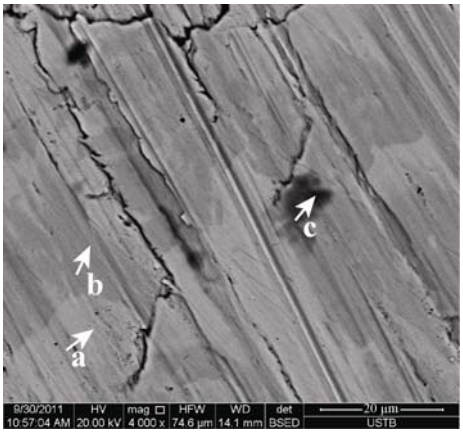

Fig. 8. SEM image of a ferronickel granule.

4. Conclusions

(1) Four mass loss steps maximized at 78, 272, 583, and 826°C are observed in the TG curve of the laterite ore, representing the vaporization of free water, the dehydroxylation of goethite, the decomposition of serpentines, and the second dehydroxylation of serpentines, respectively. XRD results reveal the complete dehydroxylation of the laterite after calcining at 900°C for 2 h.

(2) Thermal analysis shows that the reduction reactions of the graphite-laterite mixtures start at 700°C and can be divided into three major temperature regions. XRD results of the coal-laterite composites show that the reduction reactions proceed more completely at higher temperatures.

(3) Temperature has a significant effect on the growth of the reduced ferronickel particles. Metal particles with a size of about 5-10 μm are observed for the coal-laterite composite roasted at 1200°C. Obvious growth of the reduced ferronickel particles appear with the formation of worm-like crystals for the sample roasted at 1250°C, and spheric particles with sizes of 20-150 μm are observed for the sample roasted at 1300°C. When the reduction temperature increases to 1350°C, the reduced ferronickel particles agglomerate to ferronickel granules of 3-8 mm in diameter. The main elements in the granules include iron, nickel, chromium, carbon, and sulfur, in which the content of nickel is 9.08 wt.% and that of iron is 85.21 wt.%.

References

[1] Dalvi A.D., Bacon W.G., and Osbourne R.C., The past and the future of nickel laterites, [in] *PDAC 2004 International Conference Trade Show and Investors Exchange*, Toronto, 2004: 27.

[2] Kim J., Dodbiba G., Tanno H., Okaya K., Matsuo S., and Fujita T., Calcination of low-grade laterite for concentration of Ni by magnetic separation, *Miner. Eng.*, 2010, **23** (4): 282.

[3] Lee H.Y., Kim S.G., and Oh J.K., Electrochemical leaching of nickel from low-grade laterites, *Hydrometallurgy*, 2005, **77** (3-4): 263.

[4] Nayak J.C., Production of ferro-nickel from sukinda laterites in rotary kiln-electric furnace, *Trans. Indian Inst. Metall.*, 1985, **38** (3): 241.

[5] Wamer A.E.M., Dfaz C.M., Dalvi A.D., Mackey P.J., and Tarasov A.V., JOM world nonferrous smelter survey, Part III: Nickel: Laterite, *JOM*, 2006(4): 11.

[6] McDonald R.G. and Whittington B.I., Atmospheric acid leaching of nickel laterites review: Part I. Sulphuric acid technologies, *Hydrometallurgy*, 2008, **91** (1-4): 35.

[7] Kaya Ş. and Topkaya Y.A., High pressure acid leaching of a refractory lateritic nickel ore, *Miner. Eng.*, 2011, **24** (11): 1188.

[8] Valix M. and Cheung W.H., Effect of sulfur on the mineral phases of laterite ores at high temperature reduction, *Miner. Eng.*, 2002, **15** (7): 523.

[9] Power L.F. and Geiger G.H., The application of the reduction roast-ammoniacal ammonium carbonate leach to nickel latenites, *Miner. Sci.*, 1997, **9** (1): 32.

[10] Georgiou D. and Papangelakis V.G., Sulphuric acid pressure leaching of a limonitic laterite: chemistry and kinetics, *Hydrometallurgy*, 1998, **49** (1-2): 23.

[11] Guo X.Y., Li D., Park K.H., Tian Q.H., and Wu Z., Leaching behavior of metals from a limonitic nickel laterite using a sulfation-roasting-leaching process, *Hydrometallurgy*, 2009, **99** (3-4): 144.

[12] Watanabe T., Ono S., Arai H., and Matsumori T., Direct reduction of gamierite ore for production of ferronickel with a rotary kiln at Nippon Yakin Co. Ltd. Oheyama Works, *Int. J. Miner. Process.*, 1987, **19**: 173.

[13] Matsumori T., Ishizuka T., and Matsuda T., An economical smelting method of ferro-nickel as raw material of stainless steel, *Metall. Rev. MMIJ*, 1996, **13** (1): 144.

[14] Carlson L. and Schwertmann U., Natural ferrihydrites in surface deposits from Finland and their association with silica, *Geochim. Cosmochim. Acta*, 1981, **45**: 421.

[15] Swamy Y.V., Kar B.B., and Mohanty J.K., Physico-chemical characterization and sulphatization roasting of low-grade nickeliferous laterites, *Hydrometallurgy*, 2003, **69** (1-3): 89.

[16] Valix M. and Cheung W.H., Study of phase transformation of laterite ores at high temperature, *Miner. Eng.*, 2002, **15** (8): 607.

[17] Brindley G.W. and Wan H.M., Compositions, structures, and thermal behavior of nickel-containing minerals in the lizardite-nepouite series, *American Mineralogist*, 1975, **60**: 863.

[18] Tartaj P., Cerpa A., García-González M.T., and Serna C.J., Surface instability of serpentine in aqueous suspensions, *J. Colloid Interf. Sci.*, 2000, **231**, 176.